Review Article
cnj.araku.ac.ir

☑ Cite This: Colloid Nanosci. J. 3(3) (2025) 696-706 DOI: 10.61882/CNJ.3.3.696

Photocatalytic Degradation of Methylene Blue and Catalytic Reduction of 4-Nitrophenol Using Green-Synthesized Silver Nanoparticles from Orange Peel Pectin

Mohammadali Pourmohammadi Mahunaki[1]*, Mohammad Hadi Meshkatalsadat[2], Tayebeh Momeni[2]

[1]Department of Polymer Engineering, Faculty of Engineering, Qom University, Qom, Iran
[2]Department of Chemistry, Qom University of Technology, Qom, Iran

ARTICLE INFO

Article History:
Received 2025-11-27
Revised 2026-01-06
Accepted 2026-01-07
Published 2026-01-09

Corresponding Authors:
Mohammadali Pourmohammadi Mahunaki
Email:
pourmohammadi@qut.ac.ir

ABSTRACT

Environmental contamination by organic pollutants, such as dyes and nitroaromatic compounds, poses significant health and ecological risks. In this study, pectin extracted from orange peels was utilized as a green reducing and stabilizing agent for the synthesis of silver nanoparticles (AgNPs). The generated nanoparticles were characterized by X-ray diffraction (XRD), field emission scanning electron microscopy (FE-SEM), Fourier transform infrared spectroscopy (FTIR), ultraviolet-visible spectroscopy (UV-Vis), and transmission electron microscopy (TEM). The result verified the formation of uniformly spherical nanoparticles with an average size of ~20–30 nm. Then, The catalytic activity of AgNPs toward the reduction of 4-nitrophenol (4-NP) in the presence of $NaBH_4$ as a reducing agent, as well as their photocatalytic activity in the degradation of methylene blue (MB) under visible-light irradiation, were investigated separately. The results demonstrated that, in the catalytic process, nearly complete conversion of 4-NP to 4-aminophenol (4-AP) was achieved within 15 min using 1 mL of AgNPs, while complete reduction occurred within 5 min when the catalyst amount was increased to 2 mL. In contrast, in the photocatalytic process, MB was efficiently degraded in the presence of AgNPs under visible-light irradiation, with a pronounced decrease in absorption intensity observed within 25 min, and the degradation efficiency increased with increasing AgNPs dosage. This study highlights that green synthesis of AgNPs using orange peel pectin is a simple, economically and environmentally friendly methods for the synthesis of photocatalytically active nanoparticles.

KEYWORDS: *Pectin; Orange peel; Silver nanoparticles; Photocatalysis; Methylene blue; 4-Nitrophenol*

Introduction

The field of nanotechnology is becoming more and more advanced, multidisciplinary field that integrates chemistry, biology, and the science of materials. Among various nanomaterials, silver nanoparticles (AgNPs) have been extensively investigated owing to their unique electrical, optical, and biological properties. These characteristics enable a wide range of applications, including drug delivery, biosensing, imaging, catalysis, nanodevice fabrication, and biomedical technologies[1]. In particular, AgNPs exhibit strong antibacterial activity and are therefore widely used in sunscreens, cosmetics, textiles, and food-related applications [2-4]. Moreover, size-dependent interactions between AgNPs and the HIV-1 virus have been demonstrated, keeping the virus from integrating into the host cell in vitro[5]. Several physical and chemical methods have been developed for the synthesis of metal nanoparticles, such as photochemical reduction, lithography, laser ablation, ultrasonic-assisted synthesis, aerosol techniques, and UV irradiation. However, many of these approaches are costly,

energy-intensive, and often involve the use of toxic chemicals, which raise environmental and health concerns[6, 7]. Consequently, increasing attention has been directed toward environmentally friendly and sustainable synthesis strategies, commonly referred to as green synthesis. In this context, various biological systems, including plants, fungi, bacteria, and yeast, have been employed as natural reducing and stabilizing agents for the green synthesis of AgNPs [8, 9]. Among these, plant-based materials are particularly attractive due to their availability, safety, and rich phytochemical composition [10-16]. Nevertheless, despite the growing interest in green-synthesized AgNPs, a comprehensive understanding of their interactions with biological systems and their broader environmental implications remains limited. Orange peel represents an attractive and sustainable resource for the eco-friendly synthesis of silver nanoparticles. As an abundant byproduct of the juice industry, orange peel contains a high concentration of pectin, a natural polysaccharide widely distributed in the middle lamella and cell walls of higher plants, particularly fruits and vegetables. Structurally, pectin is primarily composed of galacturonic acid units, which provide functional groups capable of participating in reduction and stabilization processes during nanoparticle synthesis [17]. Commercially, natural pectin is mainly extracted from agro-industrial residues such as citrus peels and apple pomace, highlighting its availability and low cost [18]. Beyond its well-established applications in food systems as a thickening, stabilizing, and gelling agent, pectin has recently attracted increasing attention as a green reducing and capping agent in nanomaterial synthesis. The presence of hydroxyl and carboxyl functional groups in pectin enables effective interaction with metal ions, making it a promising biopolymer for sustainable nanoparticle production. [19].

Metal nanoparticles have recently emerged as effective photocatalysts for the degradation of organic dyes, owing to their high surface area and ability to promote light-induced redox reactions. Photocatalysis is considered an environmentally friendly treatment method for organic pollutants due to its high efficiency and non-selective nature compared with conventional remediation techniques [25]. Among various metal nanoparticles, AgNPs have attracted considerable attention because of their strong photocatalytic activity under light irradiation. Methylene blue (MB) is a widely used organic dye in industries such as textiles, paper, and printing, and its extensive use has resulted in serious environmental contamination. Due to its toxicity, persistence, and resistance to biodegradation, MB poses significant ecological and health risks [20]. AgNPs have demonstrated excellent potential for the photocatalytic degradation of MB, as they can generate reactive oxygen species (ROS) under light exposure. These highly reactive species are capable of oxidizing MB molecules into less harmful products, ultimately converting them into carbon dioxide and water[21]. In addition to dye degradation, nitrophenol derivatives are also major organic pollutants commonly treated using photocatalytic degradation, adsorption, and chemical reduction methods [22-24]. Among these approaches, chemical reduction is considered the most efficient pathway for transforming nitrophenols into value-added aminophenols [25]. Sodium borohydride ($NaBH_4$) is widely used as a reducing agent for this purpose; however, the reaction proceeds slowly in the absence of a catalyst [26, 27]. The presence of metal nanoparticle catalysts, such as AgNPs, significantly accelerates the reduction process. In particular, the reduction of 4-NP to 4-aminophenol (4-AP) is of great interest, as 4-AP is an important intermediate in the production of dyes, analgesics, antipyretics, and antioxidants [28].

However, despite the growing interest in green synthesis routes, there are still limited studies reporting the use of pectin extracted from orange peel as a dual-function green reducing and stabilizing agent for AgNP synthesis. Moreover, the photocatalytic performance of these biogenically synthesized AgNPs in both organic dye degradation and nitrophenol reduction has not yet been systematically investigated.

In the present study, silver nanoparticles (AgNPs) were synthesized using pectin derived from orange peel obtained from local juice industries in the northern region of Iran. The resulting nanoparticles were characterized using various analytical techniques, and their photocatalytic activity in aqueous solution was evaluated for MB photodegradation and nitrophenol reduction.

2. Material and Methods

2.1 Materials

Silver nitrate ($AgNO_3$), ethanol (96%), sodium

hydroxide, sodium borohydride, and hydrochloric acid (37%) were supplied by Merck Company. The synthesized INPs were characterized using a Shimadzu UV-160A spectrometer for UV-Vis measurements in the 200–1000 nm range and a 50 W tungsten-halogen lamp for the 400–1000 nm region. The deuterium lamp operates at ~65–90 V and 300 mA (approximate electrical power 20–30 W), a Thermo Avatar spectrometer for FT-IR analysis, and a FEI Quanta 200 TESCAN Mira-3 SEM to examine surface morphology and particle size. X-ray diffraction (XRD) analysis was performed using a Philips PW 1730 diffractometer at 2θ = 20–80° and room temperature, confirming the amorphous nature of the synthesized INPs.

2.2. Pectin extraction

50g of dried orange peel and 0.5L of dionized water are combined to create the extraction mixture. HCl is used to adjust the pH to 2, and the mixture is then sonicated for 22 minutes at 70 °C using an ultrasonic instrument (Parsonic 2600; Iran). This combination was heated to a boil for 1hr on a hot plate. Then, a 1:2 ratio of ethanol (96%) was mixed into the slurries and let to stand for about 24 hours at 25 °C. The precipitated pectin was then collected the mixture was centrifuged for five minutes at 1200 rpm and then dried in an oven set at 60 °C.

2.3. Green synthesis of silver nanoparticles (AgNPs)

This step involved adding 10g of extracted pectin and 2g of silver nitrate to 110 mL of deionized water, stirring the mixture for 30 minutes at ambient temperature until the color changed to a dark reddish brown, showing that AgNPs are forming. Next, sodium hydroxide (1N) was added, and Centrifuging the mixture at 1200 rpm/5 minutes for 24 hours. The precipitate that was left behind was cleaned twice—once with distilled water and once with alcohol—for the purpose of removing impurities before being dried at 500 °C for 10 minutes.

2.4. Photo-catalytic degradation of MB dye by AgNPs

After adding varying quantities of ground-up nanoparticles and 5 mg of MB to deionized water, the mixture was allowed to sit in the dark for approximately 2 hours. Next, the photodegradation process was tuned for catalyst concentration (20–100 mg) and duration of contact (5–25 min).

2.5. 4-NP Reduction to 4-AP

1mL of 4-NP in a quartz cell's aqueous solution. The concentration of 4-NP was varied between 4 -10 M to investigate how the starting concentration of the substrate affects the rate of reaction. Freshly prepared $NaBH_4$ solution (3-10 M, 1mL) was then used a micropipette to add to the quartz cell. For several minutes, the mixture was agitated to ensure proper homogenization. The reaction was started by adding 3 mg of the catalyst (AgNPs). The entire process was carried out under subdued lighting conditions to minimize photocatalytic effects.

3. Results and Discussion

3.1. Characterization of Pectin

3.1.1. Fourier Transform Infrared Spectroscopy (FTIR) of pectin

The FTIR spectra obtained from the extracted pectin and the spectrum of standard pectin were compared to demonstrate that pectin had peaks at 3337, 1601, 1399, 1259, and 1031 cm^{-1} (Fig. 1)[29, 30]. The main peak in the 3200-3600 cm^{-1} range demonstrates the abundance of OH groups in the pectin structure; the specific peak in wave 1601 cm^{-1} is associated with O-H bond stretching vibrations, which are primarily derived from galacturonic acid units in the pectin backbone. The band at 1399 cm^{-1} is assigned to C–H bending vibrations, particularly from –CH groups, reflecting the polysaccharide backbone structure. the distinct peak in wave 1259 cm^{-1} of non-coherent stretching vibrations associated with the C-O-C bond and signifies the quantity of methoxy groups; the specific peak in the range of 1031 cm^{-1}, confirming the polysaccharide nature of the molecule and supporting the presence of the carbohydrate backbone.

3.2. Characterization of AgNPs

3.2.1. UV–Visible spectroscopy

AgNP production can be verified and their size and morphology evaluated using the potent technique of UV-Vis spectroscopy. The 400–450 nm region that is usually where AgNPs peak is expected to be located was covered by the scan range, which was set between 300 and 600 nm [31]. An absorption peak at 419 nm was observed in the UV-Vis spectrum of the AgNPs solution, indicating the formation of silver nanoparticles (Fig. 2). This peak position in all of the plant extracts utilized for synthesis is a reliable sign of the generation of spherical AgNPs. Coherent oscillations of surface

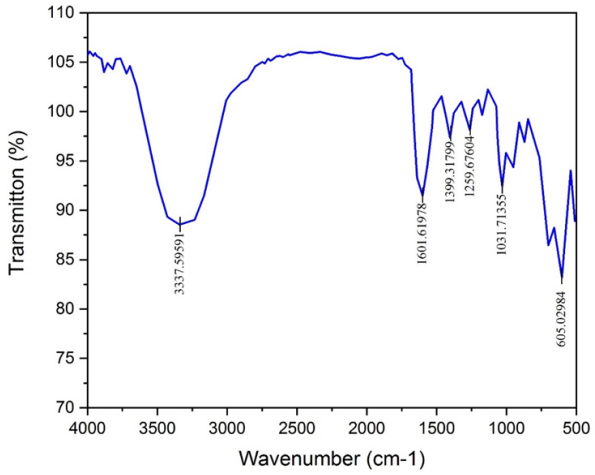

Fig. 1. FT-IR spectrum of pectin extracted from orange peel.

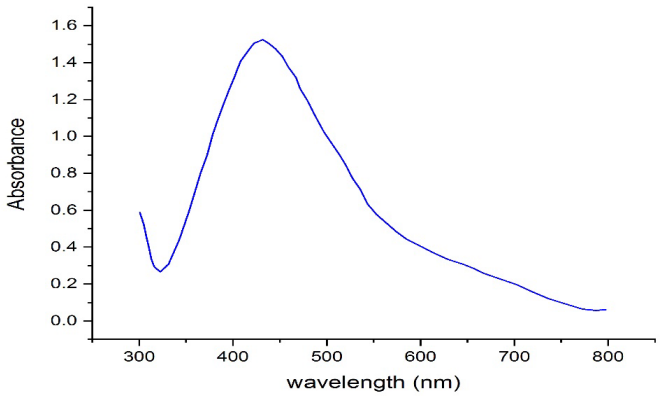

Fig. 2. UV-Vis absorption spectra of AgNPs synthesized using pectin, measured the wavelength range of 200–800 nm.

plasmons are free electrons localized on the AgNPs surface, and they are the source of the observed peak. Strong light absorption at a particular wavelength results from the electrons in these nanoparticles being activated by light [32]. The size and shape of AgNPs influence the position of the surface plasmon resonance (SPR) peak (λ_{max}). In our study, the SPR peak observed at 417nm is consistent with the formation of spherical AgNPs, as reported in previous studies[33].

3.2.2. Fourier-transform infrared spectroscopy (FT-IR)

FT-IR investigations were conducted to gather data on the chemical groups around AgNPs. In Fig. 3 showed absorption peaks at 3345.35, 2874.50, 2079.62, 1664.27, 1568.20, 1380.81, 1079.35, 939.21 and 622.933 cm^{-1}. Phenols and alcohols' O–H stretching groups are linked to this broad peak at 3345.35 cm^{-1}. The methylene (CH_2) and methyl (CH_3) groups of aliphatic compounds' C–H vibrations under stretch may be related to the peaks at 2874.50 and 2079.62 cm^{-1} [34]. The band at 1664.27 cm^{-1} might be the result of the protein's amide I band binding with the N–H stretching. All aliphatic and aromatic amines have C–N stretching vibrations that are responsible for the two bands that were found at 1380.81 and 1079.35 cm^{-1} [35]. Two bands, located at 939.21 and 622.93 cm^{-1}, demonstrated the stretch bending of amide IV (OCN) for proteins [36]. Through a reducing process, this amide I band can interact with carboxylate ions or free amine groups on Ag^{+} ions to synthesis Ag-NPs [37]. These functional

groups remain adsorbed on the AgNP surface as stabilizing (capping) agents and play a key role in catalytic electron transfer, while remaining chemically stable under photocatalytic conditions [38].

3.2.3. X-ray diffraction (XRD)

To study the crystal nanostructure of the silver nanoparticles (AgNPs), X-ray diffraction (XRD) measurements were carried out on the AgNP powder samples. In Fig. 4, The XRD pattern's diffraction peak positions were 38.070, 44.290, 64.440, and 77.340. Each peak's Miller Indices (hkl) and indexing correspond to the crystallographic lattice planes (File No. 04-0783, Joint Committee on Powder Diffraction Standards, is acceptable) and are (111), (200), (220), and (311). The intense peak at 38.07° (111) indicates a dominant polycrystalline phase with a face-centered cubic (FCC) structure, confirming the successful synthesis of crystalline AgNPs. The presence of multiple diffraction peaks at higher angles further supports the

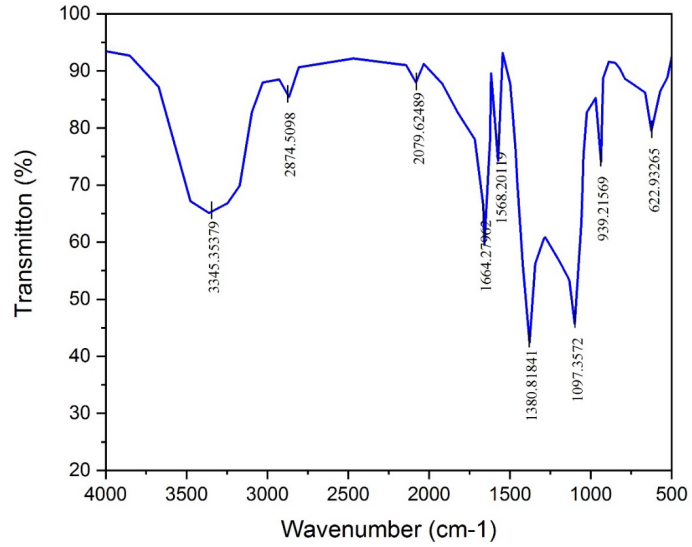

Fig. 3. FT-IR spectrum of AgNPs synthesized using pectin.

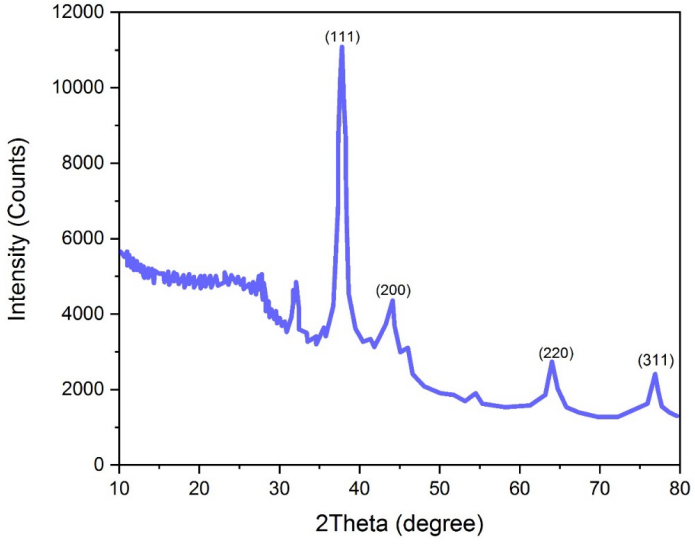

Fig. 4. XRD pattern of AgNPs synthesized using pectin.

FCC polycrystalline nature of the nanoparticles. Compared to bulk silver, the observed diffraction peaks are slightly broadened, which is commonly associated with nanoscale crystallites and indicates a reduction in particle size.Additionally, there is good agreement between the experimental (2θ) and standard (2θ) diffraction angles in Table 1 [39, 40]. AgNPs were found to have a crystallite size of 20.23 nm through the Debye-Scherrer technique calculated using the following equation 1:

$$D = \frac{0.89\lambda}{\beta \cos\theta} \quad (1)$$

As indicated in Table 1, where θ is the angle of Bragg's diffraction (° or radian) and 2θ = 38.07° corresponds to the X-ray wavelength λ = 0.154056 nm. The highest intensity peak's complete width at half maximum, or β, is known. Based on information from XRD examination, According to Table 1, The green-synthesised AgNPs have an average crystallite size of 33.82 nm.

3.2.4. Transmission electron microscopy (TEM)

Considering that nanoparticles' size and shape might change their chemical and physical properties, it is crucial to understand how they are distributed in terms of size. This leads to the pursuit of synthesis techniques that produce nanoparticles with homogeneous sizes and shapes. For this reason, one of the most effective techniques for figuring out where nanoparticles are found and analysing their size, shape, and other characteristics is transmission electron microscopy (TEM). It is significant to remember that plant-extracted green production of AgNPs was the focus of most TEM investigations. Fig. 5 displays a typical TEM image of AgNPs. In Fig. 5, the synthesized AgNPs exhibit a homogeneous morphology and spherical shape, about 21.86 ± 3.88 nm in size on average and a range of sizes from 10 to 34 nm. The absence of significant agglomeration suggests that phytochemicals present in the plant extract effectively capped and stabilized the nanoparticle surfaces, preventing excessive particle coalescence. Overall, the uniform spherical shape and size distribution observed in the TEM analysis confirm the successful synthesis of well-dispersed AgNPs and highlight the efficiency of the plant-mediated green synthesis route in producing stable silver nanoparticles with controlled nanoscale dimensions

3.2.5. Field emission scanning electron (FE-SEM)

The AgNPs, with various sizes and shapes, were analyzed using FE-SEM to gain deeper insight into nanostructured materials. The AgNPs shown in

Table 1. Using the Debye-Scherrer equation to obtain crystallite size.

2θ of intense peak	FWHM β	Miller indicates	Crystallite diameter (nm)
37.8	1.01	111	17.1
44.1	1.08	200	17.6
64.01	0.65	220	48.1
76.88	1.15	311	52.5

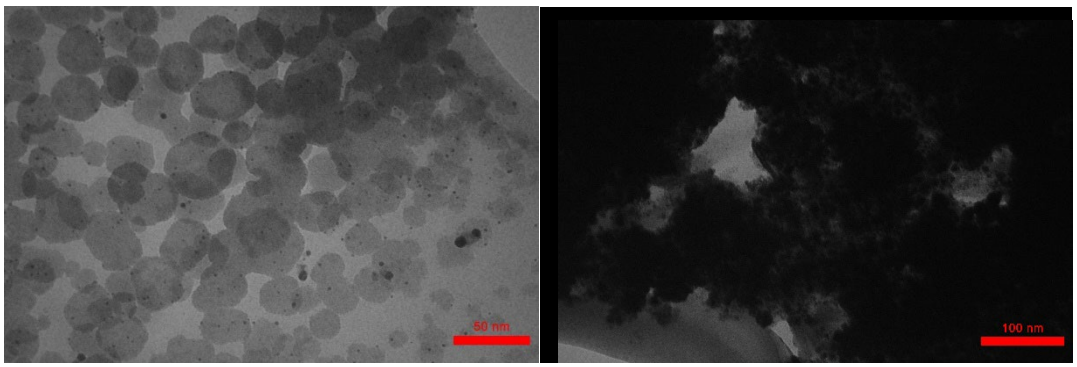

Fig. 5. TEM image of AgNPs synthesized using pectin.

Fig. 6 were synthesized using pectin extract as a reducing and stabilizing agent. . These compounds could have special qualities as compared to pure silver. Additionally, the general spherical shape of the crystal is seen. Based on the images from the FE-SEM the estimated grain size of the sample was 57.32 nm. The FESEM image shows the size of polycrystalline particles. Ag is among the majority of metals with FCC structure. AgNPs frequently aggregate due to their high surface energy, it could explain the presence of some larger nanoparticles. A major property of the generated AgNPs is catalytic activity, which is increased by their broad surface area and small particle size[41].

4. Photocatalytic activity

4.1. Photocatalytic Degradation of MB Dye by Ag-NPs

The photocatalytic effectiveness of the AgNPs with MB dye was assessed using a spectrophotometer. MB solution at constant concentration and AgNPs solutions that includes 5, 10, 15, 20, and 25 mg were were used to study AgNPs' photocatalytic effect on the degration of MB. The intensity of each solution's absorption spectrum was measured in 25 minutes through UV-Vis spectroscopy, It was shown that an increase in AgNP concentration lead to a drop in MB absorption intensity. The average number of accessible and active sites on the catalyst's surface rises as AgNPs concentration raises, which in turn causes an increase in hydroxyl radicals. Fig. 7 shows that, using the UV-Vis spectroscopic method at the maximum absorption wavelength ($\lambda_{max} \approx$ 664 nm), the intensity of the solutions' absorption spectra containing AgNPs at concentrations of 20, 40, 60, 80, and 100 mg after 5, 10, 15, 20, and 25 minutes was assessed. It was noted that the samples containing 15, 20 and 25 mg of AgNPs MB's absorption intensity has reduced as a result of the photocatalytic system's extended exposure to UV light; this suggests that the concentration of MB in the solution has dropped and that its photocatalytic breakdown has increased. An approximate degradation efficiency of 78% was achieved after 25 min under UV irradiation at the highest AgNP concentration. In addition, control experiments were carried out to verify the photocatalytic role of AgNPs. Negligible degradation of methylene blue was observed either under light irradiation without AgNPs or in the presence of AgNPs under dark conditions, confirming that the degradation occurred mainly due to the photocatalytic activity of AgNPs under UV irradiation.

4.2. Ag-NPs' catalytic actions in 4-NP reduction

We used 4-NP reduction when $NaBH_4$ is present to observe the catalytic effectiveness of AgNPs. The AgNPs act as a heterogeneous catalyst by providing active sites on their surface, facilitating electron transfer from the borohydride ions (BH_4^-) to the 4-NP ions. This electron transfer reduces the nitro group ($-NO_2$) of 4-NP to an amino group ($-NH_2$), forming 4-AP. The nanoparticles prevent direct recombination of electrons and stabilize the intermediate species, thereby accelerating the reduction reaction and enhancing catalytic efficiency. Fig. 8 showed the general schematic representation of 4-NP being reduced to 4-AP. 4-NP

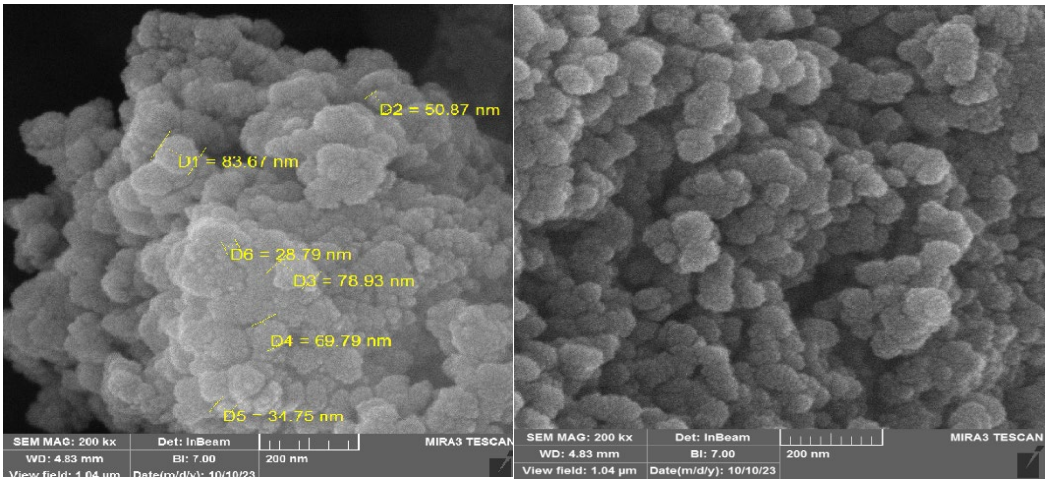

Fig. 6. FE-SEM images of AgNPs synthesized using pectin.

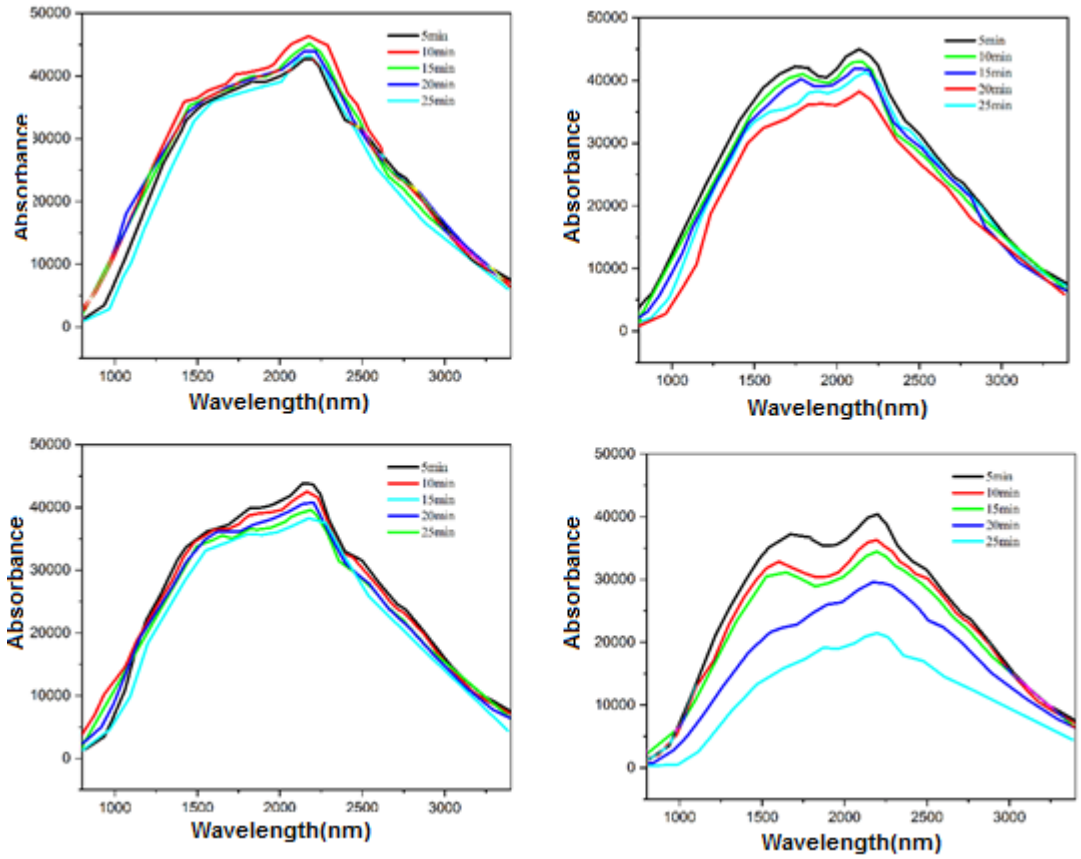

Fig. 7. UV-Vis of solutions containing (a) 5 mg, (b) 10 mg, (c) 15 mg and (d) 25 mg of AgNPs at different times Under the photocatalytic system.

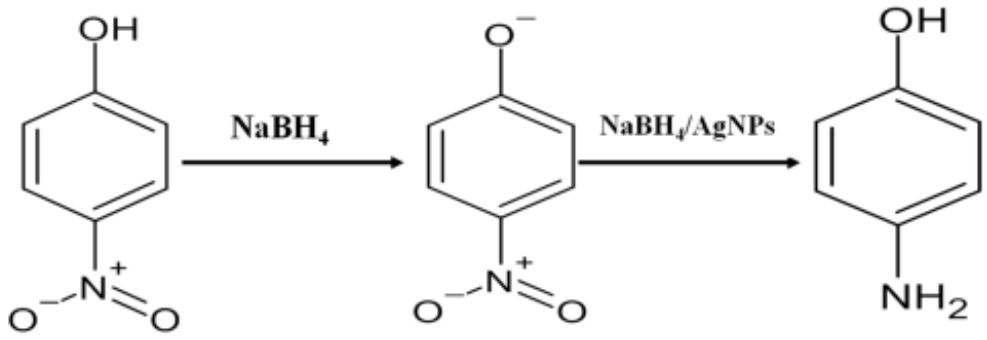

Fig. 8. Diagram showing the conversion of 4-NP to 4-AP.

formed a 4-nitrophenolate ion when $NaBH_4$ was added. At λ_{max} = 317 nm, 4-NP is reduced to 4-AP, at λ_{max} = 400 nm, the peak eventually disappears and a new peak at λ_{max} = 300 nm gradually emerges. At λ_{max} = 400 nm, Ions of 4-nitrophenolate absorb, the 4-NP shows a distinctive absorption [26]. In a blank (control) experiment, for an hour, we continuously stirred after adding 15 mL of $NaBH_4$ (0.1 M) and 15 mL of 4-NP (50 mM). As a result, we were able to see how $NaBH_4$ alone reduced 4-NP to 4-AP. The 4-nitrophenolate peak at λ_{max} = 400 nm had a very slight shift. Nevertheless, we

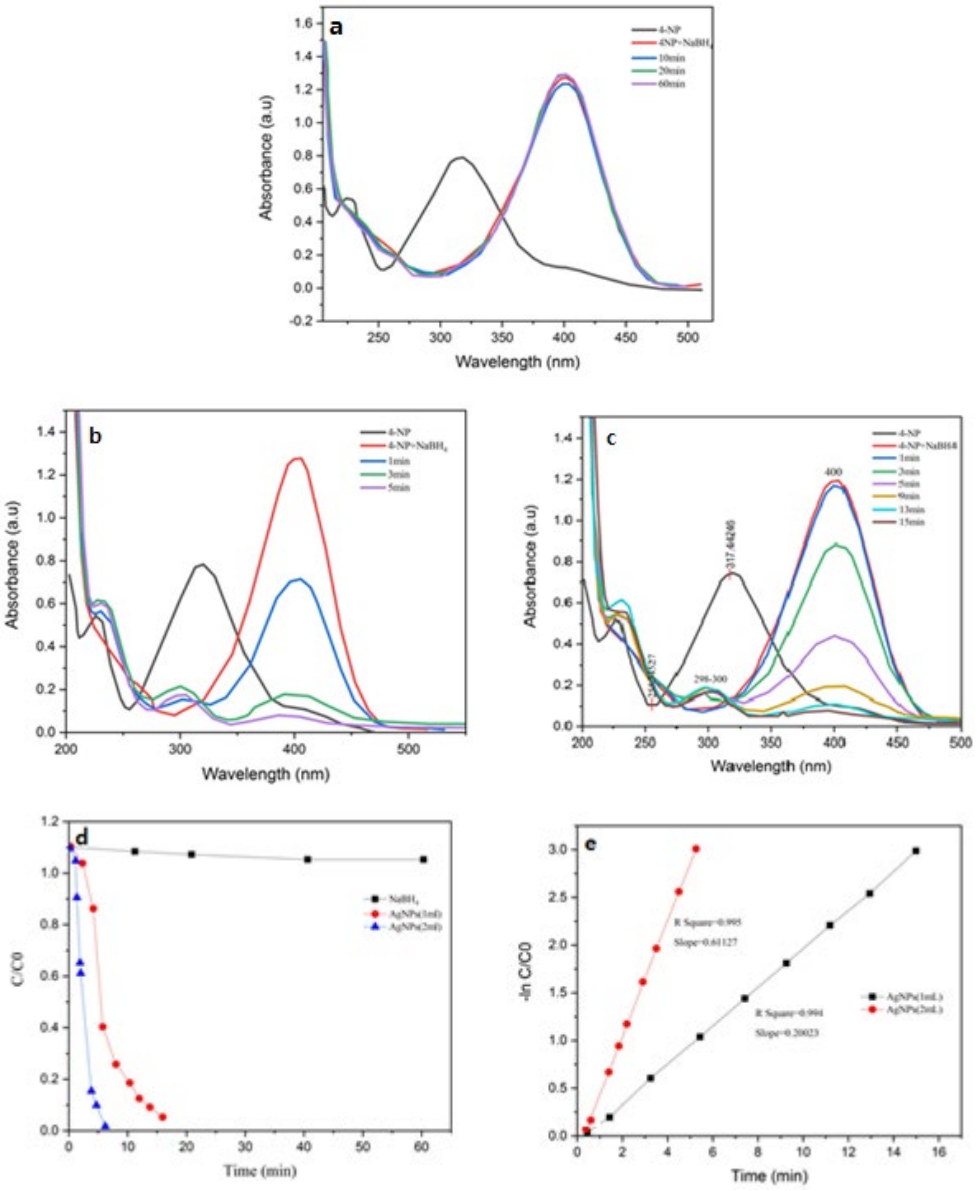

Fig. 9. Catalytic reduction of 4-nitrophenol (4-NP): (a) UV–Vis absorption spectra in the presence of $NaBH_4$, (b) UV–Vis absorption spectra in the presence of 1 mL of AgNPs, (c) UV–Vis absorption spectra in the presence of 2 mL of AgNPs, (d) concentration (C/C_0) versus reaction time, and (e) pseudo-first-order kinetic plot of $-\ln(C/C_0)$ versus time.

saw a steady drop in the λ_{max} of 4-nitrophenolate upon adding 1 mL of catalyst (AgNPs solution), along with the slow development of a peak at 298–300 nm [42]. The 4-NP solution was found to almost entirely transform into 4-AP in 15 minutes. This corresponds to an approximate reduction efficiency of about 90–95%, calculated from the decrease in absorbance at λ_{max} = 400 nm. In a related experiment, we added more catalyst, and As shown in Fig. 8, the 4-NP solution completely reduced in 5 minutes following adding 2 mL of AgNPs solution. The association between the rate of 4-NP degradation in the AgNPs and the amount of time in the solution was shown using the Langmuir-Hinshelwood model [39]. Equation (2) can be used to compute the rate of equation: The effectiveness of only $NaBH_4$ and different concentrations of the catalyst combined with $NaBH_4$ are compared using

the plot of C/C_0 vs time (in minutes) presented in Fig. 8.

A $-\ln(C/C_0)$ function of time plot was made and presented in Fig. 9 in order to examine the reaction's kinetics. The values of C/C_0 were calculated using the 400 nm decrease of λ_{max}. Based on the linear fit of the plots, catalyst amounts of 1 and 2 mL yielded coefficients of determination (R^2) of 0.994 and 0.995, respectively, indicating excellent linearity. By employing the pseudo-first-order method, the degradation of 4-NP was analyzed. . Based on the slopes of the 4-NP degradation using 1 and 2 mL of catalyst, the apparent rate constants were found to be 0.20023 and 0.61127 min^{-1}, respectively. The appearance of an absorption peak at 300 nm indicated the formation of 4-AP as the sole product of the reaction, the isosbestic spots that developed at 250, 270, and 325 nm confirmed that this investigation was further supported [26].

Conclusion

Finally, the green synthesis of AgNPs using orange peel pectin proved to be a successful approach. Comprehensive characterization techniques, including UV–Vis spectroscopy, XRD, and electron microscopy analyses, confirmed the successful formation of AgNPs with a relatively uniform size distribution and well-defined morphology. Such structural features are crucial for providing a high density of active surface sites. The synthesized AgNPs exhibited pronounced photocatalytic activity under visible light irradiation, leading to a substantial degradation of methylene blue through oxidative pathways and an efficient reduction of 4-nitrophenol via electron transfer mechanisms. This research highlights the potential of orange peel waste as a low-cost and renewable resource for the green synthesis of functional photocatalysts. The eco-friendly nature of the synthesis process, combined with the notable photocatalytic efficiency of the resulting AgNPs, suggests their practical applicability in wastewater treatment systems for the removal of organic pollutants.

Acknowledgement

The authors thank the chemistry department of Qom University of Technology and research deputy for their technical assistance with this work.

References

[1] M. Ahamed, M.M. Khan, M. Siddiqui, M.S. AlSalhi, S.A. Alrokayan, Green synthesis, characterization and evaluation of biocompatibility of silver nanoparticles, Physica E Low-dimens Sys. Nanostruct, 43 (2011) 1266-1271. https://doi.org/10.1016/j.physe.2011.02.014

[2] N. Vigneshwaran, A. Kathe, P. Varadarajan, R. Nachane, R. Balasubramanya, Functional finishing of cotton fabrics using silver nanoparticles, J. nanosci. nanotech. 7 (2007) 1893-1897. https://doi.org/10.1166/jnn.2007.737

[3] S. Kokura, O. Handa, T. Takagi, T. Ishikawa, Y. Naito, T. Yoshikawa, Silver nanoparticles as a safe preservative for use in cosmetics, Nanomed. Nanotech. Bio. Med. 6 (2010) 570-574. https://doi.org/10.1016/j.nano.2009.12.002

[4] F. Martinez-Gutierrez, P.L. Olive, A. Banuelos, E. Orrantia, N. Nino, E.M. Sanchez, F. Ruiz, H. Bach, Y. Av-Gay, Synthesis, characterization, and evaluation of antimicrobial and cytotoxic effect of silver and titanium nanoparticles, Nanomed. Nanotech. Bio. Med. 6 (2010) 681-688. https://doi.org/10.1016/j.nano.2010.02.001

[5] J. L. Elechiguerra, J. L. Burt, J.R. Morones, A. Camacho-Bragado, X. Gao, H.H. Lara, M. J. Yacaman, Interaction of silver nanoparticles with HIV-1, J. nanobiotech. 3 (2005) 1-10. https://doi.org/10.1186/1477-3155-3-6

[6] K. Okitsu, A. Yue, S. Tanabe, H. Matsumoto, Y. Yobiko, Formation of colloidal gold nanoparticles in an ultrasonic field: control of rate of gold (III) reduction and size of formed gold particles, Langmuir, 17 (2001) 7717-7720. https://doi.org/10.1021/la010414l

[7] R. R. Naik, S. J. Stringer, G. Agarwal, S. E. Jones, M. O. Stone, Biomimetic synthesis and patterning of silver nanoparticles, Nat. mater., 1 (2002) 169-172. https://doi.org/10.1038/nmat758

[8] A. Leela, M. Vivekanandan, Plant mediated synthesis of silver nanoparticles using a bryophyte Fissidens munutus and its antimicrobial activity, Afr. J. Biotechnol., 7 (2008).

[9] A. D. Dwivedi, K. Gopal, Biosynthesis of silver and gold nanoparticles using Chenopodium album leaf extract, Colloids Surf. A: Physicochem. Eng. Asp. 369 (2010) 27-33. https://doi.org/10.1016/j.colsurfa.2010.07.020

[10] H. Bar, D. K. Bhui, G. P. Sahoo, P. Sarkar, S. Pyne, A. Misra, Green synthesis of silver nanoparticles using seed extract of Jatropha curcas, Colloids Surf. A: Physicochem. Eng. Asp., 348 (2009) 212-216. https://doi.org/10.1016/j.colsurfa.2009.07.021

[11] S. S. Shankar, A. Ahmad, M. Sastry, Geranium leaf assisted biosynthesis of silver nanoparticles, Biotech. prog. 19 (2003) 1627-1631. https://doi.org/10.1021/bp034070w

[12] M. Dubey, S. Bhadauria, B. Kushwah, Green synthesis of nanosilver particles from extract of Eucalyptus hybrida (safeda) leaf, Dig. J. Nanomater. Biostruct, 4 (2009) 537-543.

[13] S. P. Dubey, M. Lahtinen, M. Sillanpää, Tansy fruit mediated greener synthesis of silver and gold nanoparticles, Process Biochem. 45 (2010) 1065-1071. https://doi.org/10.1016/j.procbio.2010.03.024

[14] N. Ahmad, S. Sharma, M. K. Alam, V. Singh, S. Shamsi, B. Mehta, A. Fatma, Rapid synthesis of silver nanoparticles using dried medicinal plant of basil, Colloids Surf B: Biointerfaces, 81 (2010) 81-86. https://doi.org/10.1016/j.colsurfb.2010.06.029

[15] D. Philip, Biosynthesis of Au, Ag and Au–Ag nanoparticles using edible mushroom extract, Spectrochimica Acta Part A: Mol Biomol Spect.73 (2009) 374-381. https://doi.org/10.1016/j.saa.2009.02.037

[16] A. Saxena, R. Tripathi, R. Singh, Biological synthesis of silver nanoparticles by using onion (Allium cepa) extract and their antibacterial activity, Dig J Nanomater Bios, 5 (2010) 427-432.

[17] L. R. Adetunji, A. Adekunle, V. Orsat, V. Raghavan, Advances in the pectin production process using novel

extraction techniques: A review, Food Hydrocoll, 62 (2017) 239-250. https://doi.org/10.1016/j.foodhyd.2016.08.015

[18] Z. J. Kermani, A. Shpigelman, H.T.T. Pham, A. M. Van Loey, M. E. Hendrickx, Functional properties of citric acid extracted mango peel pectin as related to its chemical structure, Food Hydrocoll. 44 (2015) 424-434. https://doi.org/10.1016/j.foodhyd.2014.10.018

[19] H. Bagherian, F.Z. Ashtiani, A. Fouladitajar, M. Mohtashamy, Comparisons between conventional, microwave-and ultrasound-assisted methods for extraction of pectin from grapefruit, CEP:PI. 50 (2011) 1237-1243. https://doi.org/10.1016/j.cep.2011.08.002

[20] D. Sharma, A. Kumar, N. Singh, Biomass Conversion and Biorefinery, (2022) 1-32.

[21] N. Bonnia, M. Kamaruddin, M. Nawawi, S. Ratim, H. Azlina, E. Ali, Green biosynthesis of silver nanoparticles using 'Polygonum Hydropiper'and study its catalytic degradation of methylene blue, Procedia Chem. 19 (2016) 594-602. https://doi.org/10.1016/j.proche.2016.03.058

[22] D. Vidyasagar, A. Gupta, A. Balapure, S.G. Ghugal, A.G. Shende, S.S. Umare, 2D/2D Wg-C3N4/g-C3N4 composite as "Adsorb and Shuttle" model photocatalyst for pollution mitigation,J.Photochem. Photobio. A: Chem. 370 (2019) 117-126. https://doi.org/10.1016/j.jphotochem.2018.10.038

[23] Q. Huang, M. Liu, J. Chen, Q. Wan, J. Tian, L. Huang, R. Jiang, Y. Wen, X. Zhang, Y. Wei, Facile preparation of MoS2 based polymer composites via mussel inspired chemistry and their high efficiency for removal of organic dyes, Appl. Surf. Sci. 419 (2017) 35-44. https://doi.org/10.1016/j.apsusc.2017.05.006

[24] P. Zhao, X. Feng, D. Huang, G. Yang, D. Astruc, Coord. Chem. Rev. 287 (2015) 114-136. https://doi.org/10.1016/j.ccr.2015.01.002

[25] X. Wang, Z. Zhao, D. Ou, B. Tu, D. Cui, X. Wei, M. Cheng, Highly active Ag clusters stabilized on TiO2 nanocrystals for catalytic reduction of p-nitrophenol, Appl. Surf. Sci. 385 (2016) 445-452. https://doi.org/10.1016/j.apsusc.2016.05.147

[26] P. Deka, R.C. Deka, P. Bharali, In situ generated copper nanoparticle catalyzed reduction of 4-nitrophenol, New J. Chem. 38 (2014) 1789-1793. https://doi.org/10.1039/C3NJ01589K

[27] M. Angamuthu, G. Satishkumar, M. Landau, Precisely controlled encapsulation of Fe3O4 nanoparticles in mesoporous carbon nanodisk using iron based MOF precursor for effective dye removal, Micropor. Mesopor. Mater.251 (2017) 58-68. https://doi.org/10.1016/j.micromeso.2017.05.045

[28] Y. Wei, B. Han, X. Hu, Y. Lin, X. Wang, X. Deng, Synthesis of Fe3O4 nanoparticles and their magnetic properties, Procedia Engin. 27 (2012) 632-637. https://doi.org/10.1016/j.proeng.2011.12.498

[29] M. Monsoor, U. Kalapathy, A. Proctor, Determination of polygalacturonic acid content in pectin extracts by diffuse reflectance Fourier transform infrared spectroscopy, Food Chem. 74 (2001) 233-238. https://doi.org/10.1016/S0308-8146(01)00100-5

[30] F. Kar, N. Arslan, Characterization of orange peel pectin and effect of sugars, L-ascorbic acid, ammonium persulfate, salts on viscosity of orange peel pectin solutions, Carbohydr. Polym. 40 (1999) 285-291. https://doi.org/10.1016/S0144-8617(99)00063-6

[31] M. Nasrollahzadeh, Z. Issaabadi, S.M. Sajadi, Green synthesis of the Ag/Al2O3 nanoparticles using Bryonia alba leaf extract and their catalytic application for the degradation of organic pollutants, J. Mater. Sci. Mater. Elect. 30 (2019) 3847-3859. https://doi.org/10.1007/s10854-019-00668-8

[32] M. Nasrollahzadeh, R. Akbari, Z. Issaabadi, S.M. Sajadi, Biosynthesis and characterization of Ag/MgO nanocomposite and its catalytic performance in the rapid treatment of environmental contaminants, Ceram. Int. 46 (2020) 2093-2101. https://doi.org/10.1016/j.ceramint.2019.09.191

[33] M. Pourmohammadi Mahunaki, M.H. Meshkatalsadat, T. Momeni, Green Synthesis of Silver Nanoparticles Using green algae Pectin for Efficient Photocatalytic Activity, JWNT, 10 (2025) 297-309. https://doi.org/10.22090/jwent.2025.03.005

[34] M. Hasanin, M.A. Elbahnasawy, A.M. Shehabeldine, A.H. Hashem, Ecofriendly preparation of silver nanoparticles-based nanocomposite stabilized by polysaccharides with antibacterial, antifungal and antiviral activities, BioMetals, 34 (2021) 1313-1328. https://doi.org/10.1007/s10534-021-00344-7

[35] I. Singh, Biosynthesis of silver nanoparticle from fungi, algae and bacteria, Europ. J. Biol. Res. 9 (2019) 45-56. https://doi.org/10.5281/zenodo.2617168

[36] C. Wu, S. Xu, W. Wang, Synthesis and applications of silver nanocomposites: A review, in J. Phys. Conference Series, IOP Publishing, 2021, 012216.

[37] C. V. Restrepo, C. C. Villa, Synthesis of silver nanoparticles, influence of capping agents, and dependence on size and shape: A review, Environ. Nanotechnol. Monit. Manag 15 (2021) 100428. https://doi.org/10.1016/j.enmm.2021.100428

[38] A. Sidorowicz, G. Fais, F. Desogus, F. Loy, R. Licheri, N. Lai, G. Cao, Microbial Nanoparticles in Biological Plant Protection, A. J. S. Concas, 16 (2024) 8758. https://doi.org/10.3390/ijms26062492

[39] M. P. Kainz, L. Legenstein, V. Holzer, S. Hofer, M. Kaltenegger, R. Resel, J. Simbrunner, GIDInd: an automated indexing software for grazing-incidence X-ray diffraction data, J. Appl. Crystallograph., 54 (2021) 1256-1267. https://doi.org/10.1107/S1600576721006609

[40] A. A. Dawood, A.A. Moosa, M.M. Radhi, Green synthesis of silver nanoparticles decorated with exfoliated graphite nanocomposites, Egypt. J. Chem., 65 (2022) 651-659. https://doi.org/10.21608/ejchem.2022.141183.6180

[41] M. Nasrollahzadeh, Green synthesis and catalytic properties of palladium nanoparticles for the direct reductive amination of aldehydes and hydrogenation of unsaturated ketones, New J. Chem. 38 (2014) 5544-5550. https://doi.org/10.1039/C4NJ01440E

[42] S. Yudha S, A. Falahudin, R.H. Wibowo, J. Hendri, D.O. Wicaksono, Reduction of 4-nitrophenol mediated by silver nanoparticles synthesized using aqueous leaf extract of Peronema canescens, Bull. Chem. React. Engineer. & Catal, 16 (2021) 253-259.